

# Self-Assembled Films of Hemoglobin/Laponite/Chitosan: Application for the Direct Electrochemistry and Catalysis to Hydrogen Peroxide

Dan Shan,<sup>\*,†,‡</sup> En Han,<sup>‡</sup> Huaiguo Xue,<sup>\*,†,‡</sup> and Serge Cosnier<sup>§</sup>

Key Laboratory of Environmental Materials and Environmental Engineering of Jiangsu Province, Yangzhou 225002, China, School of Chemistry and Chemical Engineering, Yangzhou University, Yangzhou 225002, China, and Laboratoire d'Electrochimie Organique et de Photochimie Rédox, UMR CNRS 5630, Institut de Chimie Moléculaire de Grenoble (FR CNRS 2607), Université Joseph Fourier, 38041 Grenoble, France

Received March 25, 2007; Revised Manuscript Received June 23, 2007

A highly stable biological film was formed on the functional glassy carbon electrode (GCE) via step-by-step self-assembly of chitosan (CHT), laponite, and hemoglobin (Hb). Cyclic voltammetry (CV) of the Hb/laponite/CHT/GCE showed a pair of stable and quasi-reversible peaks for the Hb-Fe(III)/Fe(II) redox couple at about  $-0.035$  V versus a saturated calomel electrode in pH 6.0 phosphate buffer at a scan rate of  $0.1 \text{ V s}^{-1}$ . The electrochemical reaction of Hb entrapped on the laponite/CHT self-assembled film exhibited a surface-controlled electrode process. The formal potential of the Hb-heme-Fe(III)/Fe(II) couple varied linearly with the increase of pH over the range of 3.0–8.0 with a slope of  $-63 \text{ mV pH}^{-1}$ , which implied that an electron transfer was accompanied by single-proton transfer in the electrochemical reaction. The position of the Soret absorption band of this self-assembled Hb/laponite/CHT film suggested that the entrapped Hb kept its secondary structure similar to its native state. The self-assembled film showed excellent long-term stability, the CV peak potentials kept in the same positions, and the cathodic peak currents retained 90% of their values after 60 days. The film was used as a biological catalyst to catalyze the reduction of hydrogen peroxide. The electrocatalytic response showed a linear dependence on the  $\text{H}_2\text{O}_2$  concentration ranging widely from  $6.2 \times 10^{-6}$  to  $2.55 \times 10^{-3} \text{ M}$  with a detection limit of  $6.2 \times 10^{-6} \text{ M}$  at  $3 \sigma$ .

## Introduction

Direct electron transfer between an electrode material and a redox-active protein or protein clusters has become an intriguing phenomenon for last three decades. The investigations on the direct electron-transfer process of proteins and underlying electrodes can not only help us to understand the mechanisms of redox transformations between redox biomolecules in biocatalysis and metabolic processes involving electron transportation in biological systems but also provide us a platform for fabricating biosensors, enzymatic bioreactors, and biomedical devices.<sup>1</sup> In general, the direct absorption of redox protein on the bare conventional electrode has been demonstrated to result in large changes in its conformation and often in denaturation of the protein.<sup>2,3</sup> Moreover, the extended three-dimensional structures of the protein can lead to inaccessibility of the redox sites.<sup>4</sup> Therefore, a great amount of efforts have been devoted to the modification of either the protein or the electrode surface to limit denaturing adsorption and control the orientation at the protein/electrode interface to achieve a direct rapid electron transfer.

Among many different strategies used for the modification of electrode surfaces, the self-assembly technique exhibits unprecedented flexibility to tailor interfacial properties and

present biologically relevant groups, which makes it well-suited for the control of biomolecular density and orientation at the solid–liquid interface to obtain better reproducibility and higher efficiency. Electrode materials may be functionalized by the introduction of surface groups by, for example, oxidation of carbon surfaces,<sup>5</sup> silanization of platinum electrodes, or formation of self-assembled thiolate monolayers on gold surfaces.<sup>6–8</sup> In subsequent steps, proteins and/or additional compounds necessary for establishing a fast electron transfer may be covalently linked to these primary functional sites.<sup>9</sup>

Clay colloid provides a favorable microenvironment for electron transfer and catalytic reactions on the electrode.<sup>10,11</sup> In the literature, there are several reports on direct electrochemistry based on clay–protein-modified electrodes.<sup>12–14</sup>

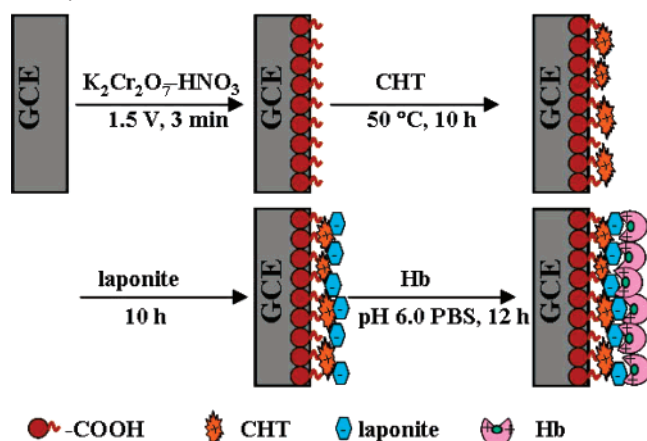
Under Association Internationale pour l'Etude des Argiles nomenclature, only natural materials can be denoted as clays, while a synthetic clay is more properly distinguished as a clay mineral.<sup>15</sup> The synthesized clay can provide control over properties such as composition, porosity, and cation exchange capacity (CEC). Laponite is a synthesized hectorite of formula of  $(\text{Mg}_{5.5}\text{Li}_{0.5})\text{Si}_4\text{O}_{10}(\text{OH})_2(\text{Na}^{+}_{0.73}\cdot n\text{H}_2\text{O})$ .<sup>16</sup> Laponite contains a 2:1 primary unit consisting of two tetrahedral silicate sheets that sandwich a central metal octahedral sheet, which is separated from another unit via electrostatic interactions that arise from exchangeable cations in hydrated interlayers. Isomorphous substitution of  $\text{Mg}^{2+}$  by  $\text{Li}^{+}$  results in a layer with an excess negative charge. This excess charge is compensated by the accumulation of counterions. When suspended in deionized water, at a concentration less than  $10 \text{ g L}^{-1}$ , a complete delamination process of the elementary laponite layers (stacked together) occurs, leading to a colloidal suspension of

\* Authors to whom correspondence should be addressed. Phone: 86-514-7975436. Fax: 86-514-7975244. E-mail: danshan@yzu.edu.cn; chhgxe@yzu.edu.cn.

<sup>†</sup> Key Laboratory of Environmental Materials and Environmental Engineering of Jiangsu Province.

<sup>‡</sup> Yangzhou University.

<sup>§</sup> Université Joseph Fourier.

**Scheme 1.** Illustration of Stepwise Self-Assembly Procedures of a Hb/Laponite/CHT-Modified GCE

negatively charged elementary platelets.<sup>17</sup> Laponite presents all of the advantages of clay such as high porosity due to the swelling phenomenon in aqueous solution, chemical inertness, good adsorption properties due to its appreciable surface area, special structural features, high cation exchange capacity, and unusual intercalation properties.<sup>18–20</sup> To the best of our knowledge, there is no report on the direct electrochemistry of redox proteins based on laponite.

Encouraged by the successful nonmanual self-assembly technique, we conceived a novel sensor architecture based on hemoglobin (Hb) assembly on the assembled laponite/chitosan film. The assembly procedure is displayed in Scheme 1. Chitosan (CHT), which is a linear copolymer of D-glucosamine and N-acetyl-D-glucosamine, was used as a scaffold in this attractive configuration. In its linear polyglucosamine chains of high molecular weight, chitosan has reactive amino and hydroxyl groups. Its amino group could react with  $\text{-COOH}$  through a dehydration reaction and covalent assembly on the electrode surface.<sup>5</sup> Its  $\text{pK}_a$  is about 6.5. In aqueous acidic media ( $\text{pH} < 6.5$ ), most of the amino groups are protonated, making chitosan a cationic water-soluble polyelectrolyte. At  $\text{pH} 6.0$ , its surface charge is positive, while laponite is negative; due to the electrostatic attraction, laponite could be anchored on the chitosan-modified electrode. Hb was chosen as a model redox protein in this system, because of its commercial availability, moderate cost, and a known and documented structure. Its isoelectric point is 7.4.<sup>21</sup> It charges positively in aqueous acid media. Therefore, it can be assembled on the negatively charged laponite film.

With the Hb/laponite/CHT-modified glassy carbon electrode (GCE), the direct electrochemistry of Hb and the effects of scan rate, pH value, long-term stability, and bio-electrocatalysis to hydrogen peroxide were described.

## Experimental Section

**Chemicals and Solvents.** Bovine erythrocyte hemoglobin (Hb) was obtained from Fluka. It was used without further purification. Chitosan (CHT,  $M_w \approx 1 \times 10^6$ ; >90% deacetylation) was obtained from Shanghai Reagent Company (China). Laponite was obtained from Rockwood Specialties, Inc. (Princeton, NJ). All other chemicals were of analytical grade and used without further purification.  $\text{H}_2\text{O}_2$  was freshly prepared before being used. Phosphate-buffered saline (PBS) was 0.025 M  $\text{K}_2\text{HPO}_4$  and  $\text{KH}_2\text{PO}_4$ , and its pH was adjusted with  $\text{H}_3\text{PO}_4$  or KOH solutions. Twice-distilled water was used through out the experiment.

**Apparatus and Procedures.** Atomic force microscopy (AFM) images were obtained with a multimode digital instrument (Veeco-DI). UV–vis measurements were carried out by using a UV-2550 UV–vis spectrophotometer. A CHI 660 electrochemical workstation (CH Instruments) was used for cyclic and amperometric voltammetry. A three-electrode cell was used with a saturated calomel electrode (SCE) as the reference electrode, a platinum foil as the counter electrode, and the modified glassy carbon electrode (GCE) (diameter of 3 mm) as the working electrode on which the Hb/laponite/CHT film and Hb/CHT film were successively immobilized. Electrolytic solutions were purged with highly purified nitrogen for at least 20 min prior to the series of experiments. A nitrogen environment was then kept over the solution in the cell to prevent the contact of the solution with oxygen.

**Construction of a Hb/Laponite/CHT-Modified GCE.** A 1.0 wt % chitosan solution was prepared by dissolving chitosan flakes in 1.0 wt% acetic acid (HAc). The laponite colloid suspension ( $1 \text{ mg mL}^{-1}$ ) was prepared by dispersing laponite in deionized water with stirring overnight. Hb was dissolved in 0.025 M PBS ( $\text{pH} 6.0$ ) with a concentration of  $3 \text{ mg mL}^{-1}$ .

Prior to use, a 3-mm-diameter GCE was polished with a polishing cloth with alumina of successively smaller particles ( $1.0 \mu\text{m}$  in diameter). Then the electrode was cleaned by ultrasonication in deionized water. After that, it was oxidized at 1.5 V for 3 min in the solution containing 10%  $\text{HNO}_3$  and 2.5%  $\text{K}_2\text{Cr}_2\text{O}_7$ , by which  $\text{-COOH}$  could be formed on the surface of the GCE. After being washed with water, the GCE was immersed into 1% CHT solution for about 10 h at  $50^\circ\text{C}$ . The resulting electrode was then dipped into laponite solutions for 10 h; finally, the laponite/CHT-modified GCE was incubated in Hb ( $\text{pH} 6.0$ ) for about 12 h to attach proteins. The resultant electrode is denoted as Hb/laponite/CHT/GCE. For comparative purposes, the Hb/CHT/GCE was fabricated following the same procedure with the absence of laponite. All of the protein electrodes were washed with water and stored in  $\text{pH} 7.0$  PBS at  $4^\circ\text{C}$  when not in use.

## Results and Discussion

**Atomic Force Microscopy Characterization.** AFM experiments were performed to better characterize the self-assembly process. The surface topologies of the bare glassy carbon and the modified surfaces via self-assembly were imaged using AFM in contact mode. All images were taken from dry surfaces at room temperature under air atmosphere. The morphology of bare glassy carbon reveals a smooth surface, characterized by the presence of polishing streaks (Figure 1A). Adsorbing a layer of CHT on the functional surface glassy carbon, the morphology seems like a sheet of silk with an irregular wrinkle (Figure 1B). The thickness of this CHT self-assembled film was ca. 53.5 nm. As shown in Figure 1C, laponite globular particles, 30–60 nm in size, were anchored on the CHT film, providing a three-dimensional structure favorable for protein adsorption. This random adsorption mechanism is driven by the electrostatic interactions. The thickness of the laponite/CHT was ca. 70.2 nm. When Hb was continually self-assembled on the laponite/CHT film, the topography was significantly different, appearing in the form of “small cubes” randomly distributed over the surface with a thickness of 133.8 nm (Figure 1D). Considering the size of Hb, which is approximately  $5.5 \times 5.5 \times 7.0 \text{ nm}^3$  and ellipsoid in shape, as well as the possibility for Hb to exist as oligomers,<sup>22</sup> it is most likely that Hb has been immobilized as an aggregate.

**UV–Vis Spectroscopic Analysis.** UV–vis spectroscopy is an effective means for monitoring the possible change of the Soret absorption band in the heme group region. The band shift may provide information on the tertiary structure of heme proteins, especially that conformational change around the heme region.<sup>23</sup> Figure 2 shows the spectra of Hb in solution (curve

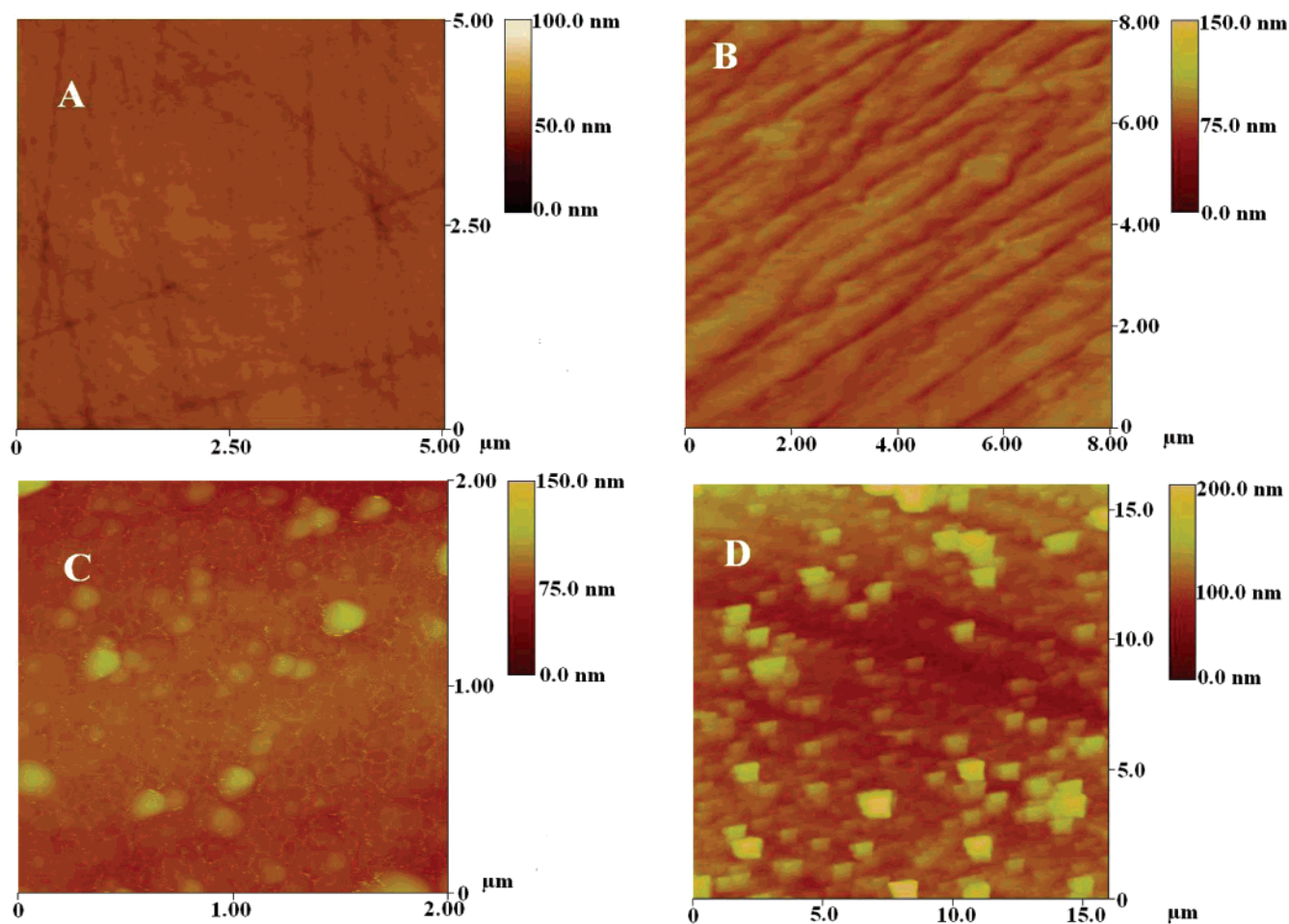


**Figure 1.** AFM images of the surfaces of (A) bare glassy carbon, (B) self-assembled CHT film, (C) self-assembled laponite/CHT film, and (D) self-assembled Hb/laponite/CHT film.

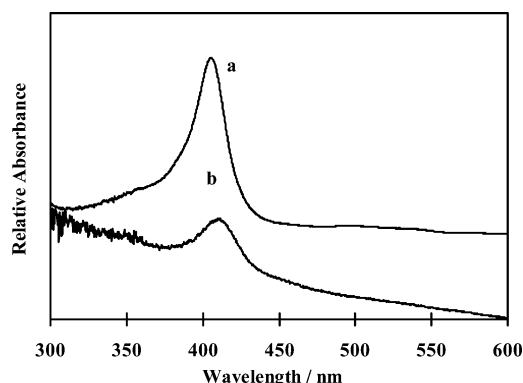


**Figure 2.** UV-vis spectra for (a) Hb in PBS (pH 6.0) and (b) Hb/laponite/CHT assembled layers on ITO glass.

a) and assembled Hb layer on laponite/CHT on indium tin oxide (ITO) glass (curve b). For Hb in PBS, the Soret band lies at 404 nm, while it is shifted to 408 nm in the laponite/CHT assembled film. The slight shift in the Soret band and the decrease in its absorbance may be due to the interaction between laponite nanoparticles and proteins for the surface potential energy and adsorption. Such interactions neither destroy the structure nor change the fundamental microenvironment of the biomolecules.

**Direct Electrochemistry of the Hb/Laponite/CHT-Modified GCEs.** *Voltammetry of Hb Assembled on the Laponite/CHT Film.* Cyclic voltammetry (CV) is especially well-suited to the study of electron-transfer kinetics of electroactive species. Figure 3 shows the cyclic voltammograms of different electrodes

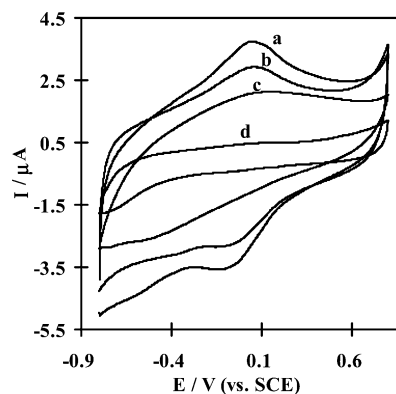


**Figure 3.** Cyclic voltammograms of (a) Hb/laponite/CHT/GCE, (b) Hb/CHT/GCE, (c) laponite/CHT/GCE, and (d) bare GCE in 0.025 M PBS (pH 6.0) at a scan rate of 0.1 V s<sup>-1</sup>.

in 0.1 M pH 6.0 PBS. The Hb/laponite/CHT/GCE gives a couple of stable and well-defined redox peaks at 0.054 and -0.125 V at 0.1 V s<sup>-1</sup> (curve a in Figure 3), while no redox peak is observable at both bare GCE (curve d in Figure 3) and laponite/CHT/GCE (curve c in Figure 3). Obviously, the response of the Hb/laponite/CHT/GCE is attributed to the redox of the electroactive centers in the assembled Hb. However, the Hb/CHT/GCE also displays a couple of redox peaks of Hb (curve b in Figure 3). However, these peak currents are smaller than those at the Hb/laponite/CHT/GCE. This phenomenon may be ascribed to the attractive electrostatic interaction between the positively charged protein shell and the negatively charged



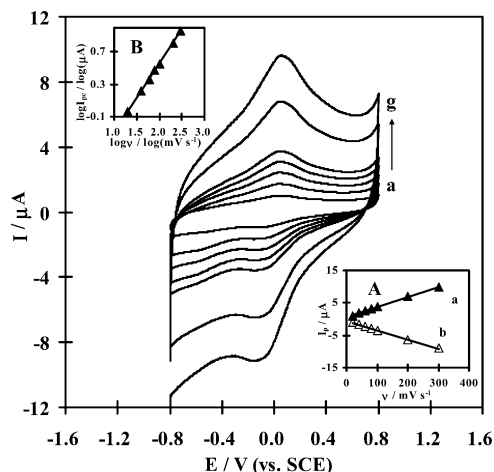


**Figure 4.** Cyclic voltammograms of the Hb/laponite/CHT/GCE in 0.025 M pH 6.0 PBS at different scan rates. The scan rates form inner to outer are (a) 20, (b) 40, (c) 60, (d) 80, (e) 100, (f) 200, and (g) 300  $\text{mV s}^{-1}$ . Inset A: The plot of anodic and cathodic peak currents vs scan rates. Inset B: Plot of logarithm of  $I_{pc}$  vs  $\log \nu$ .

laponite particles that lead to a higher amount of entrapped Hb on the laponite/CHT three-dimensional film. In contrast, positively charged CHT should lead to a repulsion of the heme edge of Hb from the electrode surface.

The peak separation ( $\Delta E_p$ , defined as  $\Delta E_p = E_{pa} - E_{pc}$ ) and the near unity ratio ( $I_{pa}/I_{pc}$ ) of anodic peak current to the cathodic one obtained on the Hb/laponite/CHT/GCE are characteristic of quasi-reversible redox process of Hb immobilized on the electrode. The formal potential ( $E^{\circ'}$ ), defined as the midpoint of reduction and oxidation potentials, is  $-0.035 \text{ V}$  for Hb, which is positive compared with that in an aqueous solution.<sup>24</sup> The formal potential difference reflected a specific influence of the different microenvironments of Hb at the surface of the electrode on  $E^{\circ'}$ . The different modified films on the electrode surface may shift the potential via interactions with the protein or by their influence on the electrode double layer.<sup>25,26</sup>

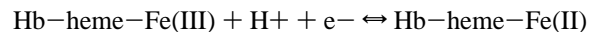
The surface coverage ( $\Gamma^*$ ) was estimated from integration of the reduction or oxidation peak of cyclic voltammograms according to  $\Gamma^* = Q/nFA$ , where  $Q$  is the charge involved in the reaction,  $n$  is the number of electrons transferred,  $F$  is the Faraday constant, and  $A$  is the electrode area.<sup>27</sup> The surface coverage ( $\Gamma^*$ ) of Hb on the surface of the laponite/CHT-modified GCE was estimated to be  $5.4 \times 10^{-10} \text{ mol cm}^{-2}$ , which was larger than  $2.1 \times 10^{-10} \text{ mol cm}^{-2}$  on Hb/GNP/ATP-ABA/GCE,<sup>28</sup>  $5.32 \times 10^{-11} \text{ mol cm}^{-2}$  on Nafion/Hb-PHEA/GCE,<sup>28</sup> and  $6.31 \times 10^{-11} \text{ mol cm}^{-2}$  on Hb-Chi-BMIM $\cdot$ BF $_4$ /GCE.<sup>30</sup> The charge under the peaks ( $Q$ ) gave a value of about  $3.7 \times 10^{-6} \text{ C}$ . On the basis of the crystallographic dimensional structure of Hb and assuming the biomolecule adopts an orientation with the long axis parallel to the electrode surface, the theoretical monolayer coverage of obtained in our experimental is thus about 29 times the theoretical monolayer coverage. This implies that a multilayer of proteins entrapped in the three-dimensional composite self-assembled film participated in the electron-transfer process. This result is consistent with that of AFM measurements.

The cyclic voltammograms of the Hb/laponite/CHT/GCE display a well-defined peak shape at different scan rates and show almost equal heights of reduction and oxidation peaks at the same scan rate (Figure 4). Peak currents vary linearly with the scan rates, as shown in the inset A of Figure 4, indicating a surface-controlled electrode process. The slope obtained by the linear regression of  $\log I_{pc}$  versus  $\log \nu$  is 0.84 for Hb (inset

B of Figure 4), which corresponded to the characteristics of a thin-layer electrochemical behavior.

**Optimization of the Hb/Laponite/CHT Self-Assembled Film.** The concentrations of components such as CHT, laponite, and Hb may have effects on the electrochemical properties of the resulting Hb/laponite/CHT self-assembled film. Thus, in this present work, a series of Hb/laponite/CHT-modified GCEs were fabricated via the self-assembly technique in different concentrations of CHT, laponite, and Hb. The electrochemical properties of these resulting modified electrodes were evaluated by CV in 0.025 M PBS (pH 6.0) at a scan rate of  $0.1 \text{ V s}^{-1}$ . The corresponding results are summarized in Table 1. It clearly appears that electrode A has the best electrochemical properties, such as the highest anodic or cathodic peak currents and relatively small peak separation. Therefore, the self-assembled Hb/laponite/CHT/GCE was fabricated in 1 wt % CHT, 1 mg/mL laponite, and 3 mg/mL Hb, respectively, in each self-assembly procedure.

**Effect of Solution pH on the Direct Electron Transfer of Assembled Hb.** Nearly reversible voltammograms with stable and well-defined peaks were obtained for the whole pH range tested (3.0–8.0) (Figure 5A). The formal potential is found to be linearly decreased with increasing pH from 3.0 to 8.0 with a slope of  $-63 \text{ mV pH}^{-1}$  (inset of Figure 5A). This value is approximately close to the theoretical value of  $-57.6 \text{ mV pH}^{-1}$  for a reversible proton-coupled single electron transfer.<sup>31</sup> This suggests that a single protonation accompanies electron transfer between the electrode and each of the four heme-Fe(III)'s of Hb, represented in general terms by



where the charges on Hb species have been omitted.

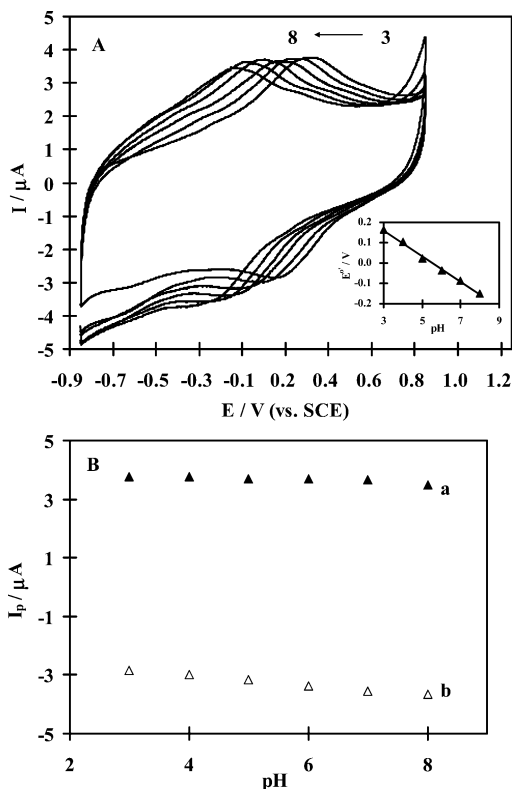
The pH value affects slightly the redox peak currents of Hb (Figure 5B). Obviously, the maximum peak currents are observed at an optimal pH range between 6.0 and 7.0. It may be due to the assembled Hb that it maintains its higher bioactivity at such a pH range.

**Stability of the Hb/Laponite/CHT/GCE.** Long-term stability is one of the most important properties required for biosensors or bioreactors. The stability of the Hb/laponite/CHT/GCE was investigated by CV. The peak height and peak potential of the surface-immobilized film over the potential range from  $-0.8$  to  $0.8 \text{ V}$  have remained nearly unchanged, and the amount of degradation after 50 cycles in buffer solution (pH 6.0) with a scan rate of  $0.1 \text{ V s}^{-1}$  was less than 1% (Figure 6A). The Hb/laponite/CHT/GCE was stored in pH 6.0 PBS, and during the whole storage time and CV tests were carried out periodically. The protein electrode exhibited excellent stability (Figure 6B). The CV peak potentials kept the same positions and the peak currents retained 90% of their values for 60 days. The excellent stability can be ascribed to the favorable electrostatic interaction between positively charged Hb and negatively charged laponite films. In addition, laponite can also provide a highly hydrophilic microenvironment for Hb to retain its native biological activity.

**Electrocatalysis of the Hb/Laponite/CHT/GCE toward  $\text{H}_2\text{O}_2$ .** Hemoglobin has a certain intrinsic peroxidase activity due to its close similarity with peroxidase, so it can be employed to catalyze the reduction of  $\text{H}_2\text{O}_2$ . Electrocatalytic reduction of  $\text{H}_2\text{O}_2$  using Hb/laponite/CHT/GCE was investigated by CV. When adding  $\text{H}_2\text{O}_2$  into a pH 6.0 buffer solution, a new reduction peak at about  $-0.6 \text{ V}$  was observed (Figures 7 d–g). However, the direct reduction of  $\text{H}_2\text{O}_2$  was not observed at laponite/CHT/GCE at the potential range from  $-1.2$  to  $0.8 \text{ V}$  (Figure 7b). Moreover, with the increase of  $\text{H}_2\text{O}_2$  concentration,

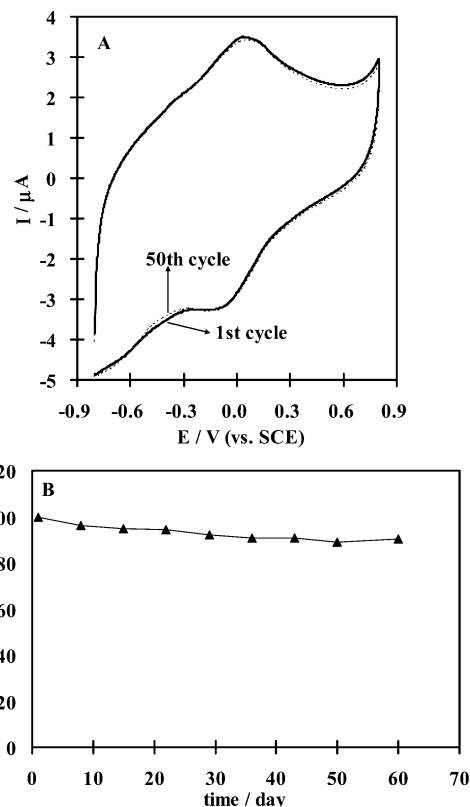
**Table 1.** Electrochemical Data Obtained from Cyclic Voltammograms of the Hb/Laponite/CHT/GCE Prepared by Self-Assembly Techniques with Different Concentrations of CHT, Laponite, or Hb<sup>a</sup>

series	Hb/laponite/CHT configuration			$I_{pa}$ ( $\mu A$ )	$I_{pc}$ ( $\mu A$ )	$I_{pa}/I_{pc}$	$E_{pa}$ (V)	$E_{pc}$ (V)	$\Delta E_p$ (V)	$E^{o'}$ (V)
	CHT (wt %)	laponite (mg/mL)	Hb (mg/mL)							
A	1	1	3	3.90	3.58	1.09	0.056	-0.127	0.183	-0.035
B	3	1	3	3.72	3.42	1.09	0.056	-0.157	0.213	-0.051
C	0.2	1	3	3.52	3.29	1.07	0.056	-0.157	0.213	-0.051
D	1	0.5	3	3.19	2.88	1.11	0.056	-0.157	0.213	-0.051
E	1	3	3	3.00	2.87	1.05	0.058	-0.157	0.215	-0.050
F	1	1	6	2.87	2.63	1.09	0.055	-0.157	0.212	-0.051
G	1	1	0.5	0.74	0.67	1.10	0.057	-0.157	0.214	-0.050

<sup>a</sup> Experiments conditions: 0.025 M PBS (pH 6.0) at a scan rate of 0.1 V s<sup>-1</sup>.**Figure 5.** (A) Cyclic voltammograms of the Hb/laponite/CHT/GCE at different pH values of 3, 4, 5, 6, 7, and 8. Scan rate: 100 mV s<sup>-1</sup>. Inset: Effect of pH on the formal potential of the Hb/laponite/CHT/GCE in 0.025 M PBS. (B) Dependence of (a) anodic and (b) cathodic peak current on the pH of the solution.

the cathodic peak current increased. According to the experimental results, it was reasonable to think that the catalytic peak around -0.6 V came from the interaction between Hb and H<sub>2</sub>O<sub>2</sub>. This result showed that the Hb/laponite/CHT film can act as an effective catalyst for the reduction of H<sub>2</sub>O<sub>2</sub>. This abnormal phenomenon of electrocatalytic reduction of H<sub>2</sub>O<sub>2</sub> by heme protein was also observed at Mb/ZrO<sub>2</sub>/CHT/GCE,<sup>5</sup> a Mb/Chit-Aus/cys self-sustained system,<sup>32</sup> and Hb/octadecylamine based on a Langmuir–Blodgett technique,<sup>33</sup> which is probably attributed to a conformational effect. The size and irregular shape of Hb and the nature of the electroactive center, in addition to their change due to the driving force of electric field, could all lead to the significant charge and spatial repulsion as the potential is scanned, resulting in the deviation from ideal behavior.<sup>34</sup>

The electrocatalytic reduction of H<sub>2</sub>O<sub>2</sub> at Hb/laponite/CHT/GCE was also studied by amperometry, which is one of the most widely employed techniques for biosensors. Figure 8

**Figure 6.** (A) First and 50th recorded cyclic voltammograms of the Hb/laponite/CHT/GCE in 0.025 M PBS (pH 6.0). Scan rate: 0.1 V s<sup>-1</sup>. (B) Long-term stability of the Hb/laponite/CHT/GCE for the redox peak currents of cyclic voltammograms.

displays the amperometric responses of different concentrations of H<sub>2</sub>O<sub>2</sub> at a Hb/CHT self-assembled film-modified electrode and a Hb/laponite/CHT self-assembled film-modified electrode with an applied potential of -0.25 V vs SCE in PBS (pH 6.0), respectively. As can be seen, the current responses at Hb/laponite/CHT/GCE are higher than those at Hb/CHT/GCE. The enhancement of current responses at Hb/laponite/CHT/GCE resulted from the laponite nanoparticle incorporation. From the steady-state current response of H<sub>2</sub>O<sub>2</sub> at the Hb/laponite/CHT/GCE, this proposed electrode achieved 95% of the steady-state current within 5 s, with a linear range from 6.2 × 10<sup>-6</sup> to 1.2 × 10<sup>-3</sup> M. The detection limit was 6.2 × 10<sup>-6</sup> M based on a signal-to-noise ratio of 3.

The apparent Michaelis–Menten constant ( $K_M^{app}$ ) can be obtained by the analysis of the slope and the intercept of the plot of the reciprocals of the steady-state current versus H<sub>2</sub>O<sub>2</sub> concentration. The  $K_M^{app}$  value for the Hb/laponite/CHT self-assembled film-modified GCE was found to be 1.09 mM, which

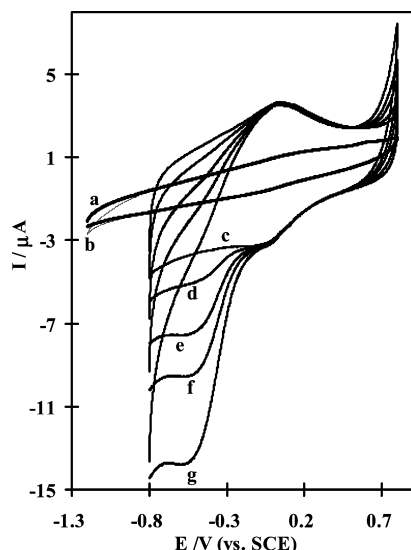


**Figure 7.** Cyclic voltammograms of (a) laponite/CHT/GCE in pH 6.0 PBS containing no  $\text{H}_2\text{O}_2$ , (b) laponite/CHT/GCE in pH 6.0 PBS containing 0.75 mM  $\text{H}_2\text{O}_2$ , (c) Hb/laponite/CHT/GCE in pH 6.0 PBS containing no  $\text{H}_2\text{O}_2$ , (d) Hb/laponite/CHT/GCE in pH 6.0 PBS containing 0.25 mM  $\text{H}_2\text{O}_2$ , (e) Hb/laponite/CHT/GCE in pH 6.0 PBS containing 0.75 mM  $\text{H}_2\text{O}_2$ , (f) Hb/laponite/CHT/GCE in pH 6.0 PBS containing 1.25 mM  $\text{H}_2\text{O}_2$ , and (g) Hb/laponite/CHT/GCE in pH 6.0 PBS containing 2.25 mM  $\text{H}_2\text{O}_2$ . Scan rate:  $0.1 \text{ V s}^{-1}$ .

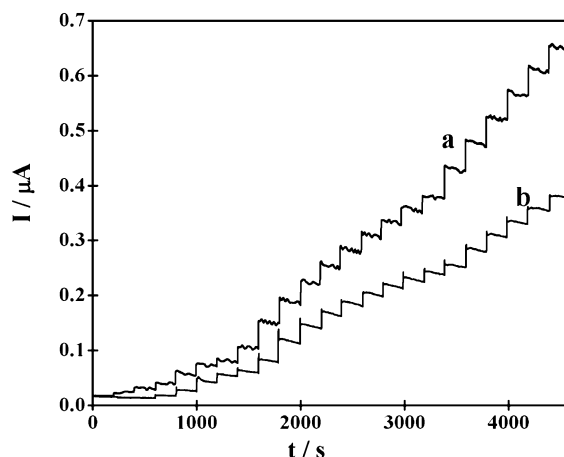


**Figure 8.** Typical steady-state responses: (a) Hb/laponite/CHT/GCE and (b) Hb/CHT/GCE on successive injection of  $\text{H}_2\text{O}_2$  into 10 mL of stirring 0.025 M PBS. Applied potential:  $-250 \text{ mV}$ .

was smaller than that obtained by Hb/Au-SBA-15 (2.87 mM),<sup>35</sup> Hb/ZrO<sub>2</sub>/CHT/GCE (1.77 mM),<sup>5</sup> and Hb/Chit-Aus/Cys/Au (1.4 mM).<sup>32</sup> Thus, the Hb self-assembled on laponite/CHT film has a high affinity for  $\text{H}_2\text{O}_2$ .

## Conclusion

In this work, we designed a novel architecture based on the self-assembled films of Hb/laponite/CHT formed step-by-step on the functional surface of a GCE. The electrostatic interaction between negatively charged laponite and positively charged Hb can enhance the affinity of the obtained films to Hb, resulting in perfect long-term stability. Moreover, it can induce more amounts loading of Hb. The electrochemical reaction of Hb assembled on the laponite/chitosan exhibited surface-controlled electrode process accompanied with one electron and one proton transportation. The immobilized Hb retained its native biological activity and high catalytic ability to  $\text{H}_2\text{O}_2$ , providing a wide

linear range from  $6.2 \times 10^{-6}$  to  $1.2 \times 10^{-3} \text{ M}$ . For the advantages of this step-by-step self-assembly technique, including the simple and nonmanual construction of the protein electrode, ordered film forming, and high stability, we anticipated that this attractive technique might have potential use in the fabrication of third generation biosensors and bioreactors.

**Acknowledgment.** The authors are grateful for the financial support of the National Natural Science Foundation of China (Grant No. 20505014), the Key Project of the Chinese Ministry of Education (Grant No. 207041), and the Foundation of the Jiangsu Provincial Key Program of Physical Chemistry at Yangzhou University.

## References and Notes

- (1) Armstrong, F. A.; Hill, H. A. O.; Walton, N. J. *Acc. Chem. Res.* **1998**, *21*, 407–413.
- (2) Reed, D. E.; Hawkridge, F. M. *Anal. Chem.* **1987**, *59*, 2334–2339.
- (3) Wang, L.; Wang, E. *Electrochem. Commun.* **2004**, *6*, 49–54.
- (4) Zhang, H. M.; Li, N. Q. *Bioelectrochemistry*. **2000**, *53*, 97–101.
- (5) Zhao, G.; Feng, J. J.; Xu, J. J.; Chen, H. Y. *Electrochem. Commun.* **2005**, *7*, 724–729.
- (6) Ferapontova, E. E.; Ruzgas, T.; Gorton, L. *Anal. Chem.* **2003**, *75*, 4841–4851.
- (7) Ding, S. J.; Chang, B. W.; Wu, C. C.; Lai, M. F.; Chang, H. C. *Anal. Chim. Acta*. **2005**, *554*, 43–51.
- (8) Ferapontova, E. E.; Gorton, L. *Bioelectrochemistry* **2005**, *66*, 55–63.
- (9) Schuhman, W. *Rev. Mol. Biotechnol.* **2002**, *82*, 425–441.
- (10) Shumyantseva, V. V.; Ivanov, Y. D.; Bistolos, N.; Scheller, F. W.; Archakov, A. I.; Wollenberger, U. *Anal. Chem.* **2004**, *76*, 6046–6052.
- (11) Liu, Y.; Liu, H.; Hu, N. *Biophys. Chem.* **2005**, *117*, 27–37.
- (12) Sun, H. *J. Porous Mater.* **2006**, *13*, 393–397.
- (13) Zhou, Y.; Hu, N.; Zeng, Y.; Rusling, J. F. *Langmuir* **2002**, *18*, 211–219.
- (14) Li, Z.; Hu, N. *J. Electroanal. Chem.* **2003**, *558*, 155–165.
- (15) Guggenheim, S.; Martin, R. T. *Clay Miner.* **1995**, *30*, 257–259.
- (16) Tanabe, K.; Misona, M.; Ono, Y.; Hattori, H. *New Solid Acids and Bases: Their Catalytic Properties*; Studies in Surface Science and Catalysis 51; Elsevier: Amsterdam, 1989.
- (17) Avery, R. G.; Ramsay, J. D. F. *J. Colloid. Interface. Sci.* **1986**, *109*, 448–454.
- (18) Mousty, C.; Cosnier, S.; Shan, D.; Mu, S. *Anal. Chim. Acta* **2001**, *443*, 1–8.
- (19) Shan, D.; Mousty, C.; Cosnier, S.; Mu, S. *J. Electroanal. Chem.* **2002**, *537*, 103–109.
- (20) Shan, D.; Mousty, C.; Cosnier, S.; Mu, S. *Electroanalysis* **2003**, *15*, 1506–1512.
- (21) Seamonds, B.; Forster, R. E.; George, P. *J. Biol. Chem.* **1971**, *246*, 5391–5397.
- (22) Nadzhafova, O.; Etienne, M.; Walcarius, A. *Electrochem. Commun.* **2007**, *9*, 1189–1195.
- (23) George, P.; Hanania, G. *J. Biochem.* **1953**, *55*, 236–243.
- (24) Song, S.; Dong, S. *Bioelectrochem. Bioenerg.* **1998**, *19*, 337–346.
- (25) Yang, J.; Hu, N.; Rusling, J. F. *J. Electroanal. Chem.* **1999**, *463*, 53–62.
- (26) Lu, Q.; Hu, S. *Chem. Phys. Lett.* **2006**, *424*, 167–171.
- (27) Murry, R. W. Chemically modified electrodes. In *Electroanalytical Chemistry*; Bard, A. J.; Ed.; Marcel Dekker: New York, 1986; Vol. 13, pp 191–386.
- (28) Zhang, L.; Jiang, X.; Wang, E.; Dong, S. *Biosens. Bioelectron.* **2005**, *21*, 337–345.
- (29) Lu, Q.; Zhou, T.; Hu, S. *Biosens. Bioelectron.* **2007**, *22*, 899–904.
- (30) Lu, X.; H. J.; Yao, X.; Wang, Z.; Li, J. *Biomacromolecules* **2006**, *7*, 975–980.
- (31) Bond, A. M. *Modern Polarographic Methods in Analytical Chemistry*; Marcel Dekker: New York, 1980.
- (32) Feng, J. J.; Zhao, G.; Xue, J. J.; Chen, H. Y. *Anal. Biochem.* **2005**, *342*, 280–286.
- (33) Yin, F.; Shin, H. K.; Kwon, Y. S. *Talanta* **2005**, *67*, 221–226.
- (34) Li, J.; Dong, S. *J. Electroanal. Chem.* **1997**, *431*, 19–22.
- (35) Xian, Y.; Xian, Y.; Zhou, L.; Wu, F.; Ling, Y.; Jin, L. *Electrochem. Commun.* **2007**, *9*, 142–148.